ACS OMEGA

Open Access

http://pubs.acs.org/journal/acsodf

Article

Adsorption Performance and Mechanisms of Tetracycline on Clay Minerals in Estuaries and Nearby Coastal Areas

Jiaxiang Shang, Mingjian Huang, Liyang Zhao, Peixi He, Yan Liu,* Honghui Pan, Shaohua Cao,* and Xixiang Liu*

Cite This: *ACS Omega* 2024, 9, 692−699

Read Online

ACCESS | Metrics & More | Article Recommendations

ABSTRACT: Clay minerals in sediments have strong adsorption capacities for pollutants, but their role in the distribution of antibiotics in estuaries and nearby coastal areas is unclear. We evaluated the clay mineral montmorillonite (SWy-2) adsorption capacity for tetracycline (TC). We assessed the adsorption capacity of SWy-2 for TC by measuring the removal percentage of 30 mg/L TC over time. The effects of pH and ionic strength on the TC adsorption onto SWy-2 were investigated. We analyzed the kinetics of TC adsorption using a pseudo-second-order model and determined the adsorption isotherm using the Langmuir equation. SWy-2 particles were characterized using zeta potential, Fourier transform infrared (FTIR), and X-ray diffraction (XRD) analyses before and after TC adsorption. The removal percentage of 30 mg/L TC by SWy-2 reached 70.76% within 0.25 h and gradually increased to 78.64% at 6 h. TC adsorption was influenced by pH and ionic strength, where low pH enhanced and high ionic strength reduced the adsorption. The kinetics of TC adsorption followed a pseudo-second-order model, and the adsorption isotherm adhered to the Langmuir equation. The saturated adsorption capacity (q_{max}) of SWy-2 for TC was 227.27 mg/g. Zeta potential, FTIR, and XRD analyses confirmed that electrostatic interactions and chemical bonds played a significant role in the TC adsorption by SWy-2. SWy-2 clay mineral exhibits a substantial adsorption capacity for TC, indicating its potential as an effective sorbent to mitigate antibiotic contamination in estuaries and nearby coastal areas. The observed effects of pH and ionic strength on TC adsorption have implications for the environmental fate and transport of antibiotics. The pseudo-second-order kinetic model and Langmuir isotherm equation provide valuable insights into the adsorption behavior and capacity of TC on SWy-2. Characterization analyses support the involvement of electrostatic interactions and chemical bonds in the SWy-2−TC adsorption mechanism.

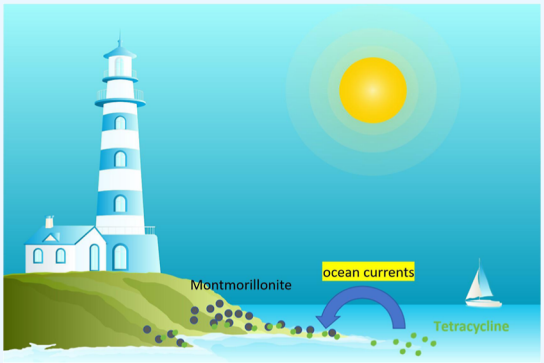

1. INTRODUCTION

Estuaries and nearby coastal areas are terrestrial−aquatic transitional zones and are highly populated and vulnerable to human activities.[1] These areas are exposed to various pollutants, including antibiotics, originating from domestic and industrial wastewater, posing a significant threat to the ecological environment of estuaries.[2] The emergence of antibiotics as a prominent pollutant further exacerbates the situation, driven by excessive medical antibiotics use and the rapid expansion of animal husbandry and aquaculture industries in China.[3,4] China, in particular, accounts for a substantial portion of the global antibiotic consumption, which has steadily risen over the years.[5,6] The migration of residual antibiotics from inland sources to estuaries and nearby coastal areas occurs primarily through river systems, accumulating in these areas.[7−9] Apart from the potential consequences of inducing bacterial resistance and disrupting microbial communities in these ecological habitats, the presence of antibiotics poses a significant concern for human health throughout the food chain.[10−12] Therefore, understanding the distribution, migration, and transformation of antibiotics in estuaries and nearby coastal areas is crucial to sustainable development and preservation of these ecosystems.

Various studies have focused on the prevalence of antibiotics in estuary and nearshore environments and demonstrated their presence in domestic estuaries and nearby coastal area waterbodies.[13−15] The fate of antibiotics in water bodies is primarily determined by their interaction with suspended particles and sediments and through abiotic and biological transformations. Additionally, antibiotics can also accumulate within aquatic organisms through a process called bioaccumu-

Received: August 30, 2023
Revised: November 23, 2023
Accepted: November 24, 2023
Published: December 22, 2023

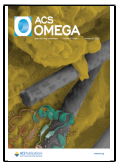

lation.[16−20] In estuarine and coastal environments, sediments serve as significant sinks for antibiotics, which accumulate due to their adsorption onto sediment particles. Recent research studies, such as those by refs 21−24, have detected antibiotics in various estuarine and nearshore sediments. Clay minerals, a crucial component of sediments found in estuaries and nearby coastal regions,[25,26] possess a large specific surface area and exhibit strong ion exchange capabilities.

Consequently, it can be inferred that the presence of clay minerals in sediment plays a crucial role in the adsorption of antibiotics. A previous study has reported a positive correlation between the content of clay minerals in sediment and the adsorption coefficient of antibiotics.[27] Although many studies have been conducted on the adsorption of antibiotics by clay minerals and modified clay minerals,[28−30] they predominantly focus on research pertaining to wastewater treatment. Nevertheless, the impact of clay minerals in sediments on the migration of TC, specifically, remains poorly understood. Hence, it is imperative to conduct further research to investigate and comprehend the interaction between antibiotics and clay minerals present in estuary and coastal sediments.

This study focused on TC, a common antibiotic that has a ubiquitous presence in the surface sediments of estuaries and coastal areas,[31] and SWy-2, a representative clay mineral that belongs to the 2:1 phyllosilicate group and is widely distributed in the environment. The primary objectives were to understand the influence of clay minerals on antibiotic adsorption in sediments. Additionally, the study aimed to characterize SWy-2 before and after TC adsorption to elucidate the mechanisms involved in the adsorption process. The study also aimed to explore the adsorption capacity of TC and investigate potential adsorption mechanisms under realistic conditions.

2. MATERIALS AND METHODS

2.1. Reagents and Materials. TC, hydrochloric acid, sodium hydroxide, and oxalic acid were purchased from Sinopharm Chemical Reagent Co., Ltd. (Shanghai, China). The SWy-2, an iron-poor smectite and ubiquitous natural clay mineral, was purchased from the Source Clays Repository of the Clay Minerals Society (West Lafayette, IN, USA). The SWy-2 particles were milled, passed through a 200 mesh sieve (0.074 mm), and then stored for use. Deionized (DI) water (18.2 mΩ cm) was obtained from a Heal Force NW ultrapure water system (Shanghai, China). All of the other chemicals used in the study were of analytical grade.

Two water and two sediment samples were taken from the Beibu Gulf, located northwest of the South China Sea and surrounded by the Leizhou Peninsula, Qiongzhou Strait, Hainan Island, Vietnam, and the Guangxi Zhuang Autonomous Region. The first set of two samples (water sample 1, labeled as W1; sediment sample 1, labeled as S1) was taken from the estuaries of Maoling River (21.8859°N, 108.4721°E); the second set of two samples (water sample 2, labeled as W2; sediment sample 2, labeled as S2) was taken from the nearby coastal areas of the Maowei Sea (21.8592°N, 108.6009°E). The samples were then transported to the laboratory and refrigerated in the dark at −20 °C.

2.2. Absorption Experiments. *2.2.1. Adsorption of TC onto SWy-2.* The absorption of TC onto SWy-2 was tested in a 250 mL glass vial. A vial was filled with 0.05 g of SWy-2 and 70 mL of DI water. Then, 30 mL of 100 mg L^{-1} TC was added to the vial to form an initial concentration of 30 mg L^{-1}. The vial was then stirred with a magnetic stirrer at 25 °C in the dark. At different time intervals (0−12 h), 0.5 mL of the suspension was extracted for analysis. The experiments on the absorption of TC in the actual water by SWy-2 and the absorption of TC by the actual sediments were conducted using the abovementioned method. Each experiment was conducted in duplicate.

The adsorption capacity (Q, mg·g^{-1}) and removal percentage (R, %) of the adsorbents for TC were calculated by eqs 1 and 2

$$Q = (C_0 - C_t)V/m \quad (1)$$

$$R=1 - C_t/C_0 \quad (2)$$

where C_0 (mg·L^{-1}) and C_t (mg·L^{-1}) are the concentrations of TC at the initial stage and time t, v (mL) is the initial solution volume, and m (g) is the adsorbent dose.

2.2.2. Effect of pH on the Adsorption of TC onto SWy-2. The effect of pH on the adsorption of TC onto SWy-2 was tested in a 250 mL glass vial. A vial was filled with 0.05 g of SWy-2 and 70 mL of DI water. Then, 30 mL of 100 mg L^{-1} TC was added to the vial to form an initial concentration of 30 mg L^{-1}. 0.1 M HCl and 0.1 M NaOH were added dropwise to adjust the pH to 2, 4, 6, 8, and 10. The vial was then stirred with a magnetic stirrer at 25 °C in the dark. At different time intervals (0−6 h), 0.5 mL of the suspension was extracted for analysis. Each experiment was carried out in duplicate.

2.2.3. Effect of Ionic Strength on the Adsorption of TC onto SWy-2. The effect of the ionic strength on the adsorption of TC onto SWy-2 was tested in a 250 mL glass vial. A vial was filled with 0.05 g of SWy-2, 68 mL of DI water, and 30 mL of 100 mg L^{-1} TC. Then, 2 mL of 0.5 M NaCl was added to the vial to form 0.01 M NaCl. The preparation of 0.05 and 0.1 M NaCl followed the same steps. The vial was then stirred with a magnetic stirrer at 25 °C in the dark. At different time intervals (0−6 h), 0.5 mL of the suspension was extracted for analysis. Each experiment was conducted in duplicate.

2.2.4. Kinetics of Adsorption of TC onto SWy-2. The absorption of TC was tested in a 250 mL glass vial. A vial was filled with 0.05 g of SWy-2 and 70 mL of DI water. Then, 30 mL of 100 mg L^{-1} TC was added to the vial to form an initial concentration of 30 mg L^{-1}. The vial was then stirred with a magnetic stirrer at 25 °C in the dark. At different time intervals (0−6 h), 0.5 mL of the suspension was extracted for analysis. Each experiment was conducted in duplicate.

2.2.5. Adsorption Isotherms of TC onto SWy-2. The absorption of TC was tested in a 250 mL glass vial. A vial was filled with 0.05 g of SWy-2 and 90, 80, 70, 60, 50, 40, and 30 mL of DI water, respectively. Then, 10, 20, 30, 40, 50, 60, 70, and 80 mL of 300 mg L^{-1} TC were added to the vial to form final concentrations of 30, 60, 90, 120, 150, 180, 210, and 240 mg L^{-1} TC, respectively. The vial was then stirred with a magnetic stirrer at 25 °C in the dark. At 6 h, 0.5 mL of the suspension was extracted for analysis. Each experiment was conducted in duplicate.

2.3. Analysis. TC adsorption was measured using an LC-16 HPLC instrument (Shimadzu, Kyoto, Japan) equipped with a UV detector and an Inter Sustain C18 column (4.6 × 250 mm). The mobile phase was a mixture of 0.01 mol/L oxalic acid, methanol, and acetonitrile (volume ratio 75:12.5:12.5) at a flow rate of 1 mL/min; the column temperature was 35 °C; and the detection wavelength was 360 nm.

https://doi.org/10.1021/acsomega.3c06478
ACS Omega 2024, 9, 692−699

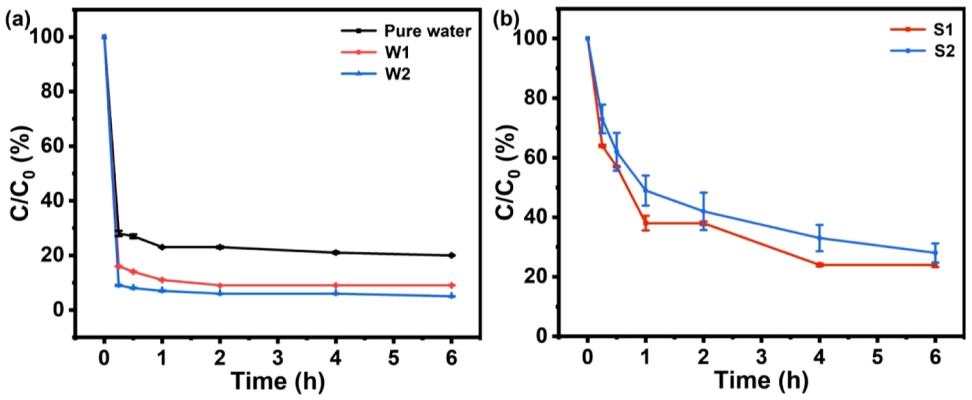

Figure 1. Absorption of TC in actual water by SWy-2 (a); and absorption of TC by actual sediments (b). Experimental conditions: 0.5 g/L SWy-2 and TC concentration in pure water, W1 and W2 were 30 mg/L respectively, the concentration of both S1 and S2 was 5 g/L, and the pH was not adjusted.

2.4. Characterization. The stability and surface charge properties of SWy-2 particles were determined using a Zeta potential analyzer Nano ZS90 (Malvern Instruments Ltd., Malvern, UK). The Fourier transform infrared (FTIR) spectroscopy of SWy-2 particles before and after absorption was performed by an FTIR spectrometer (MAGNA-1R550, Thermo Scientific, Waltham, MA, USA). X-ray diffraction (XRD) characterization analysis was used to determine the crystal structure and phase composition of SWy-2 particles before and after absorption in sediments by using an XRD testing instrument (MiniFlex 600, Rigaku, Tokyo, Japan). The whole scanning speed was set to 10°/min, and the test range was 3−80°

3. RESULTS AND DISCUSSION

3.1. Adsorption of TC under Actual Conditions. TC absorption under actual conditions was investigated by using actual water and sediment samples obtained from the Beibu Gulf. Figure 1a shows that the removal percentage of TC in actual water samples W1 and W2 by SWy-2 was significantly higher (91 and 95%, respectively) compared to the absorption in pure water by SWy-2 (80%). This can be attributed to the presence of colloidal substances in the actual water samples, which enhance the adsorption capacity of TC.

Furthermore, we investigated the adsorption of TC by actual sediment samples S1 and S2. As shown in Figure 1b, the removal percentage of TC by sediment samples S1 and S2 by SWy-2 reached 72 and 76%, respectively, and both sediment samples exhibited favorable adsorption abilities for TC. The equilibrium adsorption capacities of sediments S1 and S2 for TC at a concentration of 30 mg/L were 45.78 and 43.07 mg/g, respectively. XRD analysis of sediments S1 and S2 revealed that montmorillonite, an Fe-containing mineral, was the predominant clay mineral (as shown in Figure 2). It is worth noting that XRD analysis has limitations, and there may be other clay minerals present, such as chlorite or mica, in concentrations too low to be identified by XRD. Nonetheless, the findings support that clay minerals in sediments, including smectite, play a crucial role in the adsorption of TC. Therefore, clay minerals in sediments can be considered significant environmental sinks for antibiotic pollutants in estuaries and nearby coastal regions.

These results underscore the significant impact of clay minerals in sediments on the environmental fate of antibiotics in estuaries and nearby coastal areas. Therefore, we need to further study the adsorption capacity and mechanism of TC onto SWy-2.

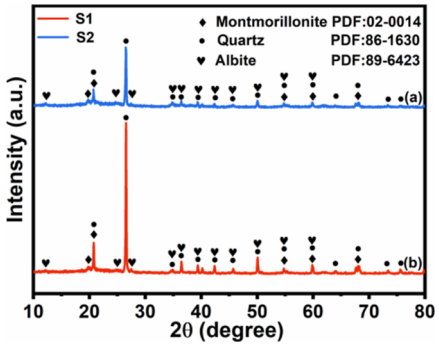

Figure 2. XRD patterns of the selected sediments. Curve A refers to the sediment S1 from the Maoling River, and Curve B refers to the sediment S2 from the Maowei Sea.

3.2. Adsorption of TC onto SWy-2. To investigate the adsorption of TC onto SWy-2, SWy-2 was used to adsorb 30 mg/L of TC. As shown in Figure 3, at predetermined time

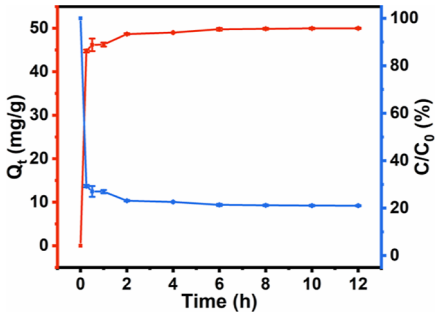

Figure 3. Adsorption capacity and the removal percentage of TC absorbed by SWy-2. Experimental conditions: 0.5 g/L SWy-2 and 30 mg/L TC; pH was not adjusted.

intervals (0−0.25 h), the removal percentage of TC quickly reached 70.76% and then continued to slowly increase until it reached 78.99% at 12 h. The adsorption equilibrium time was 6 h. Therefore, the time intervals of TC adsorption in other experiments were 0−6 h. This time profile reflected an initially quick absorption followed by a slow process, which was consistent with the previously reported two-stage feature for the absorption of substances by clay minerals.[32] At equilibrium,

https://doi.org/10.1021/acsomega.3c06478
ACS Omega 2024, 9, 692−699

the adsorption capacity of TC on SWy-2 was 50.08 mg/g. The results revealed that the clay minerals were efficient in the adsorption of TC.

3.3. Effect of pH on the Adsorption of TC onto SWy-2.

The effects of pH (2−10) on the adsorption of TC onto SWy-2 are presented in Figure 4. As the pH increased, the

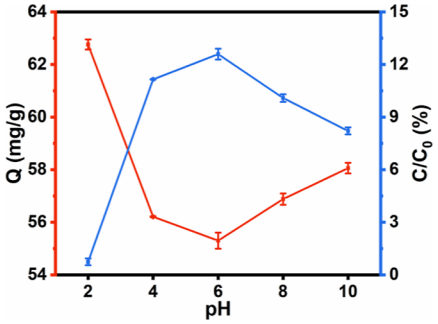

Figure 4. Effect of the pH on the adsorption of TC onto SWy-2. Experimental conditions: 0.5 g/L SWy-2 and 30 mg/L TC; pH values were adjusted to 2, 4, 6, 8, and 10.

adsorption quantity of TC decreased. The turning point appeared at pH 6, and then there was a slight increase when the pH was higher than 6. This trend showed that the affinity of TC for the SWy-2 surface was higher at a lower (acidic) pH.

The pH of the solution affected the adsorption of TC onto SWy-2, which could be attributed to the ionic structure of TC. The ionization constants pK_{a1} and pK_{a2} of TC are 3.30 and 7.68, respectively.[33] As shown in Figure 4, at pH 3.3, TC exists in the cationic form of TCH_3^+, where electrostatic attraction occurs between negatively charged SWy-2 and prevailing positively charged TCH_3^+ species. With the increase in pH, the negative charge on TC continued to intensify. Adsorption of TC onto SWy-2 occurred mainly through the cation exchange between TC and the inner and outer surfaces of SWy-2; thus, TC adsorbed onto negatively charged SWy-2 through electrostatic interactions. Therefore, as the negative charge density of TC increased, the adsorption performance of TC onto SWy-2 gradually weakened. Although optimal adsorption was achieved at a lower pH, SWy-2 still exhibited high adsorption capacities across the pH range of 2−10, indicating that SWy-2 can be an effective adsorbent of TC across an extensive pH range in natural habitats. In fact, due to the weak alkalinity of seawater and its tendency for pH values to 8, it can be inferred that clay minerals exhibit good adsorption capabilities for TC in estuaries and nearby coastal areas.

3.4. Effect of Ionic Strength on the Adsorption of TC onto SWy-2.

To assess the impact of clay minerals on TC absorption in marine environments, we conducted a study to examine the effect of ionic strength on the adsorption of TC onto SWy-2. As depicted in Figure 5, the quantity of TC adsorbed onto SWy-2 gradually decreased with increasing concentrations of NaCl. When the NaCl concentration ranged from 0 to 0.10 M, the removal percentage of TC declined from 78.99 to 39.86%. This observation suggests that competitive adsorption exists between Na^+ and TC. As the concentration of NaCl increased, the dominance of Na^+ in the competitive adsorption process grew. Consequently, Na^+ was rapidly adsorbed onto the surface of SWy-2, significantly reducing the number of available sites for TC absorption on SWy-2. Accordingly, the amount of TC adsorbed by SWy-2

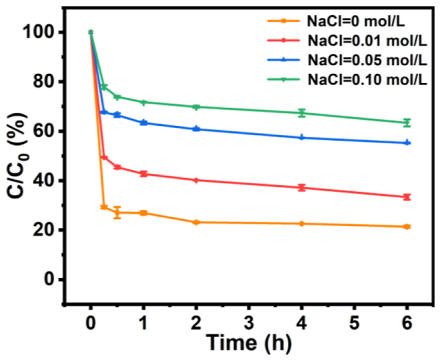

Figure 5. Effect of ionic strength on the adsorption of TC onto SWy-2. Experimental conditions: 0.5 g/L SWy-2 and 30 mg/L TC; the concentration of NaCl was 0.01, 0.05, and 0.1 M, respectively.

diminished considerably. These findings indicate that higher cation concentrations in the solution lead to lower adsorption capacities of TC by SWy-2. Considering that the salinity of seawater is typically high and it is affected by different seasons and sea area, the average value of salinity in seawater is 3.5%, which is approximately 200 times that of fresh water. So, it is crucial to acknowledge the influence of ionic strength when evaluating the impact of clay minerals on TC migration in marine and estuarine environments.

3.5. Kinetics of the Adsorption of TC onto SWy-2.

To investigate the adsorption kinetics of TC onto SWy-2, pseudo-first-order and pseudo-second-order kinetic models were employed to fit the experimental data. The dynamic models are as follows (eqs 3 and 4)

$$\ln(q_e - q_t) = \mathrm{In}q_e - k_1 t \tag{3}$$

$$\frac{t}{q_t} = \frac{1}{k_2 q_e^{\,2}} + \frac{1}{q_e} t \tag{4}$$

where q_e(mg/g) is the adsorption capacity of TC at adsorption equilibrium and q_t (mg/g) is the adsorption capacity of TC at time t. k_1(1/min) and k_2[g/(mg·min)] are the rate constants of the pseudo-first-order and the pseudo-second-order kinetic models, respectively.

The fitting results of the adsorption kinetics of TC onto SWy-2 are displayed in Figure 6b, and the corresponding dynamic parameters are shown in Table 1. By comparing the correlation coefficients of the pseudo-first-order (R^2 = 0.011) and the pseudo-second-order kinetic equations (R^2 = 0.999), we found that the adsorption process of TC by SWy-2 conformed to the pseudo-second-order kinetic model. The theoretical equilibrium adsorption capacity of TC was 50.60 mg/g under the pseudo-second-order kinetic model of the adsorption of TC onto SWy-2, and this value was close to the equilibrium adsorption capacity of 53.02 mg/g obtained during the test. These results confirmed that the adsorption of TC onto SWy-2 followed the pseudo-second-order kinetic equation, confirming that the adsorption of TC onto SWy-2 primarily occurred through physicochemical adsorption. Therefore, our study demonstrated that various physicochemical effects such as layer spacing change, covalent bond formation, and electron exchange mainly influence the adsorption process of TC onto SWy-2.

3.6. Adsorption Isotherms of TC onto SWy-2.

To further explore the adsorption isotherms of TC onto SWy-2,

https://doi.org/10.1021/acsomega.3c06478
ACS Omega 2024, 9, 692−699

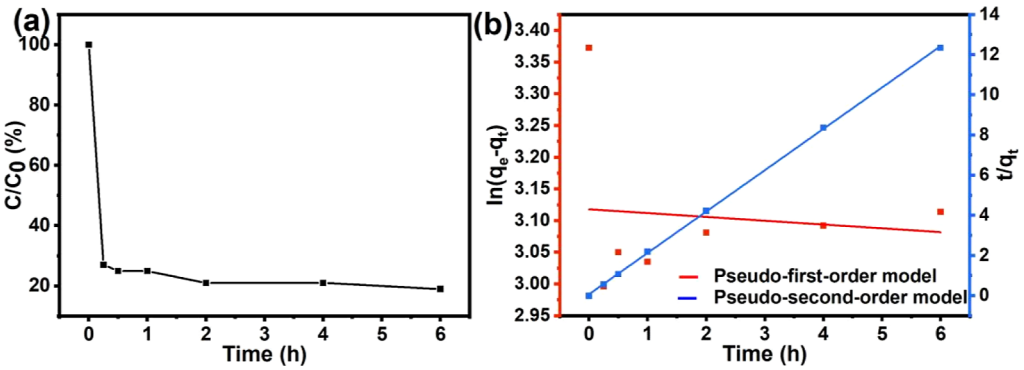

Figure 6. Adsorption of TC as a function of time (a) and the pseudo-first-order and pseudo-second-order models for TC adsorption. (b) Experimental conditions: 0.5 g/L SWy-2 and 30 mg/L TC; pH was not adjusted.

Table 1. Kinetic Parameters for TC Adsorption on SWy-2

pseudo-first-order			pseudo-second-order		
k_1(1/min)	q_e(mg/g)	R^2	k_1(g/(mg·min))	q_e(mg/g)	R^2
0.00602	22.60	0.011	0.0086	50.60	0.999

Table 2. Fitted Parameters of the Langmuir and Freundlich Equation for TC Adsorption onto SWy-2

Freundlich equation			Langmuir equation		
K_F	n	R^2	K_L	q_{max}	R^2
31.19	2.40	0.932	0.063	227.27	0.997

the Langmuir eq 5 and Freundlich eq 6 were used to fit the experimental adsorption data

$$\frac{C_e}{q_e} = \frac{C_e}{q_m} + \frac{1}{q_m K_L} \quad (5)$$

$$\ln q_e = \ln K_F + \frac{1}{n}\ln c_e \quad (6)$$

where q_e(mg/g) is the adsorption capacity of TC in the adsorption equilibrium and q_m (mg/g) is the maximum adsorption capacity of TC absorbed by SWy-2. C_e (mg/L) is the TC equilibrium concentration. K_F and K_L are the Freundlich and Langmuir adsorption constants, respectively. n is a nonideal parameter that ranges from 0 to 1 (ideal).

The fitting results are shown in Figure 7, and the fitted parameters of the Langmuir and Freundlich equation for TC adsorption onto SWy-2 are shown in Table 2. Based on the fitting results, the correlation coefficients, R^2, of the Langmuir isotherm adsorption equation and the Freundlich isotherm adsorption equation were 0.997 and 0.932, respectively. This shows that the adsorption isotherm of TC absorbed by SWy-2 was more consistent with the Langmuir isotherm equation. Therefore, it can be confirmed that the adsorption of TC onto SWy-2 was a homogeneous monolayer adsorption. In this process, TC was uniformly adsorbed on the surface of SWy-2 until it finally reached equilibrium. According to the fitting results of the Langmuir isotherm adsorption equation, the saturated adsorption capacity of SWy-2 for TC is q_{max} = 227.27 mg/g. Compared with other substances in the natural environment, the adsorption capacity of SWy-2 is relatively high. Considering that organic carbon is an important component of soils and sediments, it is necessary to compare the TC adsorption capacity of SWy-2 with that of organic carbon. Biochar is rich in organic carbon and can represent the organic carbon in soils and sediments, and the maximum adsorption capacity of Biochar derived from rice waste for TC is q_{max} = 94.63 mg/g,[34] which is lower than that of SWy-2. It reveals that clay mineral is the important environmental fate of TC versus other materials in the sediments.

The adsorption capacity of clay minerals and their specific surface area and ion exchange properties make them capable of retaining and accumulating antibiotics. Consequently, clay

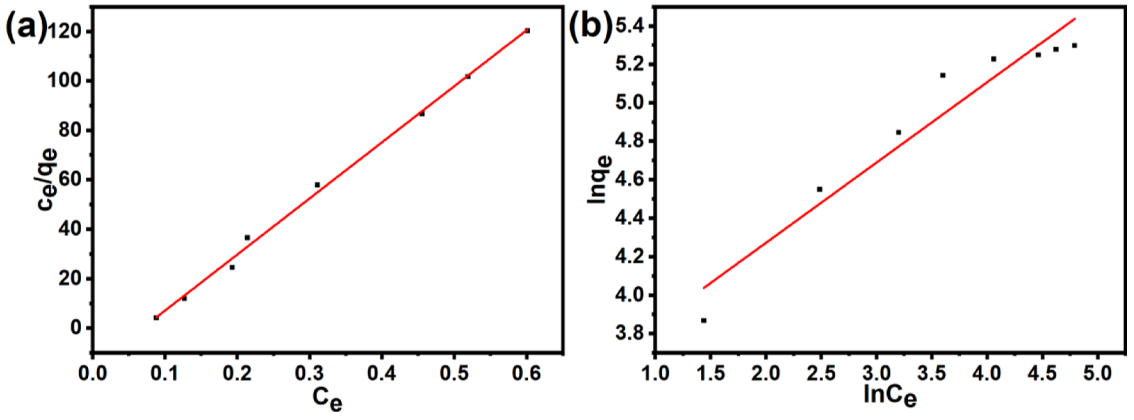

Figure 7. Adsorption isotherms of TC on SWy-2. The data were fitted using the Langmuir isotherm equation (a) and Freundlich isotherm equation (b). Experimental conditions: 0.5 g/L SWy-2, and 30, 60, 90, 120, 150, 180, 210, and 240 mg L^{-1} TC; pH was not adjusted.

https://doi.org/10.1021/acsomega.3c06478
ACS Omega 2024, 9, 692−699

minerals are potentially important sinks for antibiotic pollutants in these aquatic environments.

3.7. Mechanisms of Adsorption of TC onto SWy-2. *3.7.1. Zeta Potential of the Adsorption of TC onto SWy-2.* The variation in the zeta potential of the SWy-2 suspension liquid while SWy-2 adsorbed TC is shown in Figure 8. The

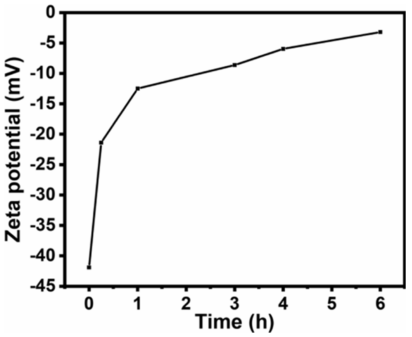

Figure 8. Zeta potential of the adsorption of TC onto SWy-2. Experimental conditions: 0.5 g/L SWy-2 and 30 mg/LTC; pH was not adjusted.

zeta potential value was negative at the time intervals 0−6 h, which was indicative of the negative surface charge of SWy-2. As shown in Figure 8, the zeta potential value of the SWy-2 suspension liquid varied considerably at 0−0.25 h intervals, which was consistent with the removal percentage of TC adsorbed by SWy-2. The results showed that the adsorption of TC by SWy-2 at a certain interval (i.e., 0−0.25 h) predominantly occurred via electrostatic interactions between the negative charge of the SWy-2 suspension liquid and the cations of TC. However, the zeta potential value of the SWy-2 suspension liquid changed slowly at intervals of 0.25−6 h, indicating that the adsorption rate was relatively slow and confirming that the adsorption of TC onto SWy-2 gradually reached equilibrium.

3.7.2. FTIR of SWy-2 Particles before and after Absorption. To further confirm the adsorption mechanism of TC by SWy-2, SWy-2 particles after TC adsorption were washed with deionized water, freeze-dried, and subsequently used to perform an FTIR test. As shown in Figure 9, compared with the infrared spectrum of pristine SWy-2, two new infrared absorption peaks appeared at 1454 and 1508 cm^{-1} after TC had been adsorbed by SWy-2 for 10 and 30 min, respectively, and the intensity of the new infrared absorption peaks

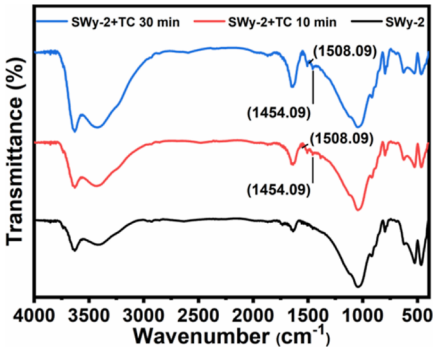

Figure 9. FTIR of SWy-2 particles before and after absorption. Experimental conditions: 0.5 g/L SWy-2 and 30 mg/L TC; pH was not adjusted.

increased as the absorption time increased. The two new infrared absorption peaks are the characteristic absorption peaks of TC. Among them, 1454 cm^{-1} is the absorption peak of NH_2 in TC, and 1508 cm^{-1} is the stretching vibration peak of the benzene ring (C═C) in TC. Accordingly, it is possible that the adsorption of TC by SWy-2 initially occurs through electrostatic interactions. The charged surface of SWy-2 attracts polar TC molecules, facilitating their adsorption. As the adsorption process progresses, chemical bonds may form between SWy-2 and TC, such as hydrogen bonds or ion−dipole interactions. These bonds contribute to the strong binding and stability of the TC−SWy-2 complex.

3.7.3. XRD of SWy-2 Particles before and after Absorption. Figure 10 shows the XRD analysis of SWy-2 in

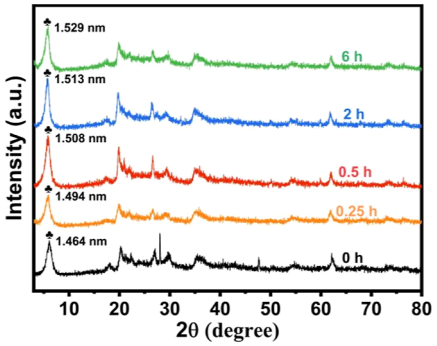

Figure 10. XRD of SWy-2 particles before and after absorption. Experimental conditions: 0.5 g/L SWy-2 and 30 mg/L TC; pH was not adjusted.

its original state and at different adsorption times. Before adsorption, the 001 diffraction peak of pristine SWy-2 was sharp and symmetrical, indicating that the pristine SWy-2 was relatively pure, exhibiting an orderly structure and good crystallinity. After adsorption, the peak pattern of SWy-2 particles did not change, but the 001 diffraction peak became stronger. This may be due to the layer spacing of SWy-2 becoming larger for TC to enter the intercalation of SWy-2. According to the Bragg formula, the crystal plane spacing of SWy-2 particles before and after absorption increased from 1.464 to 1.529 nm. During the absorption of TC by SWy-2 over time intervals of 0−6 h, the crystal plane spacing of SWy-2 particles rapidly increased from 1.464 to 1.493 nm within the first 0−0.25 h. Subsequently, the crystal plane spacing slowly increased from 1.493 to 1.529 nm from 0.25 to 6 h. These changes in crystal plane spacing corresponded well with the observed removal percentages of TC. Within the initial 0−0.25 h, the removal percentage quickly reached 70.76% and then gradually increased to 78.64% over the subsequent 0.25−6 h period, as illustrated in Figure 3. Furthermore, following adsorption, the primary diffraction peak pattern of the SWy-2 particles remained largely unchanged. This consistency can be attributed to the relatively consistent directional arrangement of TC between the layers of SWy-2.

4. CONCLUSIONS

This study utilized SWy-2 as a clay mineral model to investigate its role in the absorption of common antibiotics, specifically TC. The findings demonstrated that SWy-2 exhibited rapid adsorption of TC in the initial stages, with a slower rate of adsorption observed in the later stages. The

https://doi.org/10.1021/acsomega.3c06478
ACS Omega 2024, 9, 692−699

influence of the pH and ionic strength on TC adsorption onto SWy-2 was also examined. Low pH increased the quantity of TC adsorbed onto SWy-2, while high ionic strength decreased the adsorption capacity. The adsorption kinetics of TC onto SWy-2 followed a pseudo-second-order model, while the adsorption isotherm fit well with the Langmuir equation. The Langmuir isotherm fitting revealed a saturated adsorption capacity (q_{max}) of 227.27 mg/g for TC onto SWy-2. Various characterization techniques were used to elucidate the mechanisms underlying the adsorption of TC onto SWy-2. We found that the adsorption of TC by SWy-2 occurred mainly through electrostatic interactions, followed by the formation of chemical bonds between SWy-2 and TC. In conclusion, clay minerals, exemplified by SWy-2, demonstrated effective adsorption capabilities for typical antibiotics such as TC. Consequently, when assessing the ecological risk of antibiotics in estuarine and near-shore environments, the beneficial role of clay minerals in antibiotic adsorption should be considered.

AUTHOR INFORMATION

Corresponding Authors

Yan Liu − *Guangxi Colleges and Universities Key Laboratory of Environmental-friendly Materialsand New Technology For Carbon Neutralization, Guangxi Key Laboratory of Advanced Structural Materials and Carbon Neutralization, School of Materials and Environment, Guangxi Minzu University, Nanning 530006, China*; Email: 104812671@qq.com

Shaohua Cao − *State Environmental Protection Key Laboratory of Soil Environmental Management and Pollution Control, Nanjing Institute of Environmental Sciences, Ministry of Ecology and Environment of China, Nanjing 210042 Jiangsu, China*; Email: csh@nies.org

Xixiang Liu − *Guangxi Colleges and Universities Key Laboratory of Environmental-friendly Materialsand New Technology For Carbon Neutralization, Guangxi Key Laboratory of Advanced Structural Materials and Carbon Neutralization, School of Materials and Environment, Guangxi Minzu University, Nanning 530006, China; Guangxi Research Institute of Chemical Industry Co., Ltd., Nanning 530001, China*; orcid.org/0000-0002-8289-3206; Email: liuxx200208@163.com

Authors

Jiaxiang Shang − *Guangxi Colleges and Universities Key Laboratory of Environmental-friendly Materialsand New Technology For Carbon Neutralization, Guangxi Key Laboratory of Advanced Structural Materials and Carbon Neutralization, School of Materials and Environment, Guangxi Minzu University, Nanning 530006, China*

Mingjian Huang − *Guangxi Colleges and Universities Key Laboratory of Environmental-friendly Materialsand New Technology For Carbon Neutralization, Guangxi Key Laboratory of Advanced Structural Materials and Carbon Neutralization, School of Materials and Environment, Guangxi Minzu University, Nanning 530006, China*

Liyang Zhao − *Guangxi Colleges and Universities Key Laboratory of Environmental-friendly Materialsand New Technology For Carbon Neutralization, Guangxi Key Laboratory of Advanced Structural Materials and Carbon Neutralization, School of Materials and Environment, Guangxi Minzu University, Nanning 530006, China*

Peixi He − *Guangxi Colleges and Universities Key Laboratory of Environmental-friendly Materialsand New Technology For Carbon Neutralization, Guangxi Key Laboratory of Advanced Structural Materials and Carbon Neutralization, School of Materials and Environment, Guangxi Minzu University, Nanning 530006, China*

Honghui Pan − *Guangxi Colleges and Universities Key Laboratory of Environmental-friendly Materialsand New Technology For Carbon Neutralization, Guangxi Key Laboratory of Advanced Structural Materials and Carbon Neutralization, School of Materials and Environment, Guangxi Minzu University, Nanning 530006, China*

Complete contact information is available at: https://pubs.acs.org/10.1021/acsomega.3c06478

Author Contributions

Y.L., S.C., and X.L. planned, supervised, prepared, and edited the manuscript. J.S., M.H., L.Z., P.H., and H.P. executed the work. All authors contributed to the article and approved the submitted version.

Notes

The authors declare no competing financial interest.

ACKNOWLEDGMENTS

This work was supported by the Natural Science Foundation of China (no. 41967030), the Guangxi Natural Science Foundation (2020GXNSFAA159170), the Basic Ability Improvement Project for Young and Middle-Aged Teachers in Guangxi Province (no. 2019KY0180), and the Young Scholar Innovation Team of Guangxi Minzu University (2022).

REFERENCES

(1) Sazykin, I. S.; Khmelevtsova, L. E.; Seliverstova, E. Y.; Sazykina, M. A. Effect of antibiotics used in animal husbandry on the distribution of bacterial drug resistance (Review). *Appl. Biochem. Microbiol.* **2021**, *57*, 20−30.

(2) Beg, M. U.; Al-Muzaini, S.; Saeed, T.; Jacob, P. G.; Beg, K. R.; Al-Bahloul, M.; et al. Chemical contamination and toxicity of sediment from a coastal area receiving industrial effluents in Kuwait. Arch. *Arch. Environ. Contam. Toxicol.* **2001**, *41*, 289−297.

(3) Hossain, A.; Habibullah-Al-Mamun, M.; Nagano, I.; Masunaga, S.; Kitazawa, D.; Matsuda, H. Antibiotics, antibiotic-resistant bacteria, and resistance genes in aquaculture: risks, current concern, and future thinking. *Environ. Sci. Pollut. Res. Int.* **2022**, *29*, 11054−11075.

(4) Li, F. R.; Mai, Z. M.; Qiu, C.; Long, L. J.; Hu, A. Y.; Huang, S. J. Dissemination of antibiotic resistance genes from the Pearl River Estuary to adjacent coastal areas. *Mar. Environ. Res.* **2023**, *188*, 105978.

(5) Zhang, Q. Q.; Ying, G. G.; Pan, C. G.; Liu, Y. S.; Zhao, J. L. Comprehensive evaluation of antibiotics emission and fate in the river basins of China: source analysis, multimedia modeling, and linkage to bacterial resistance. *Environ. Sci. Technol.* **2015**, *49*, 6772−6782.

(6) Lulijwa, R.; Rupia, E. J.; Alfaro, A. C. Antibiotic use in aquaculture, policies and regulation, health and environmental risks: a review of the top 15 major producers. *Rev. Aquac.* **2020**, *12*, 640−663.

(7) Martinez, J. L. Environmental pollution by antibiotics and by antibiotic resistance determinants. *Environ. Pollut.* **2009**, *157*, 2893−2902.

(8) Niu, Z. G.; Zhang, K.; Zhang, Y. Occurrence and distribution of antibiotic resistance genes in the coastal area of the Bohai Bay, China. *Mar. Pollut. Bull.* **2016**, *107*, 245−250.

(9) Limbu, S. M.; Chen, L. Q.; Zhang, M. L.; Du, Z. Y. A global analysis on the systemic effects of antibiotics in cultured fish and their

potential human health risk: a review. *Rev. Aquac.* **2021**, *13* (2), 1015−1059.
(10) Lu, J.; Wu, J.; Zhang, C.; Zhang, Y.; Lin, Y.; Luo, Y. Occurrence, distribution, and ecological-health risks of selected antibiotics in coastal waters along the coastline of China. *Sci. Total Environ.* **2018**, *644*, 1469−1476.
(11) Xie, H. J.; Wang, X. P.; Chen, J. W.; Li, X. H.; Jia, G.; Zou, Y.; Zhang, Y.; Cui, Y. Occurrence, distribution and ecological risks of antibiotics and pesticides in coastal waters around Liaodong Peninsula, China. *Sci. Total Environ.* **2019**, *656*, 946−951.
(12) Wu, Q.; Xiao, S. K.; Pan, C. G.; Yin, C.; Wang, Y. H.; Yu, K. F. Occurrence, source apportionment and risk assessment of antibiotics in water and sediment from the subtropical Beibu Gulf, South China. *Sci. Total Environ.* **2022**, *806*, 150439.
(13) Zou, S. C.; Xu, W. H.; Zhang, R. J.; Tang, J. H.; Chen, Y. J.; Zhang, G. Occurrence and distribution of antibiotics in coastal water of the Bohai Bay, China: impacts of river discharge and aquaculture activities. *Environ. Pollut.* **2011**, *159*, 2913−2920.
(14) Zheng, Q.; Zhang, R. J.; Wang, Y. H.; Pan, X. H.; Tang, J. H.; Zhang, G. Occurrence and distribution of antibiotics in the Beibu Gulf, China: impacts of river discharge and aquaculture activities. *Mar. Environ. Res.* **2012**, *78*, 26−33.
(15) Yan, C. X.; Yang, Y.; Zhou, J. L.; Liu, M.; Nie, M. H.; Shi, H.; Gu, L. Antibiotics in the surface water of the Yangtze Estuary: occurrence, distribution and risk assessment. *Environ. Pollut.* **2013**, *175*, 22−29.
(16) Xu, X. R.; Li, X. Y. Sorption and desorption of antibiotic tetracycline on marine sediments. *Chemosphere* **2010**, *78*, 430−436.
(17) Deng, Y.; Mao, Y. P.; Li, B.; Yang, C.; Zhang, T. Aerobic Degradation of Sulfadiazine by Arthrobacter spp.: Kinetics, Pathways, and Genomic Characterization. *Environ. Sci. Technol.* **2016**, *50*, 9566−9575.
(18) Wang, J. Q.; Chen, J. W.; Qiao, X. L.; Zhang, Y. N.; Uddin, M.; Guo, Z. Y. Disparate effects of DOM extracted from coastal seawaters and freshwaters on photodegradation of 2,4-Dihydroxybenzophenone. *Water Res.* **2019**, *151*, 280−287.
(19) Zhao, Q.; Fang, Q.; Liu, H. Y.; Li, Y. J.; Cui, H. S.; Zhang, B. J.; Tian, S. Halide-specific enhancement of photodegradation for sulfadiazine in estuarine waters: Roles of halogen radicals and main water constituents. *Water Res.* **2019**, *160*, 209−216.
(20) Han, Q. F.; Zhang, X. R.; Xu, X. Y.; Wang, X. L.; Yuan, X. Z.; Ding, Z. J.; Zhao, S.; Wang, S. Antibiotics in marine aquaculture farms surrounding Laizhou Bay, Bohai Sea: Distribution characteristics considering various culture modes and organism species. *Sci. Total Environ.* **2021**, *760*, 143863.
(21) Yang, J. F.; Ying, G. G.; Zhao, J. L.; Tao, R.; Su, H. C.; Chen, F. Simultaneous determination of four classes of antibiotics in sediments of the Pearl Rivers using RRLC-MS/MS. *Sci. Total Environ.* **2010**, *408*, 3424−3432.
(22) Shi, H.; Yang, Y.; Liu, M.; Yan, C.; Yue, H. Y.; Zhou, J. L. Occurrence and distribution of antibiotics in the surface sediments of the Yangtze Estuary and nearby coastal areas. *Mar. Pollut. Bull.* **2014**, *83*, 317−323.
(23) Chen, H.; Liu, S.; Xu, X. R.; Zhou, G. J.; Liu, S. S.; Yue, W. Z.; Sun, K. F.; Ying, G. G. Antibiotics in the coastal environment of the Hailing Bay region, South China Sea: Spatial distribution, source analysis and ecological risks. *Mar. Pollut. Bull.* **2015**, *95*, 365−373.
(24) Han, Q. F.; Zhao, S.; Zhang, X. R.; Wang, X. L.; Song, C.; Wang, S. G. Distribution, combined pollution and risk assessment of antibiotics in typical marine aquaculture farms surrounding the Yellow Sea, North China. *Environ. Int.* **2020**, *138*, 105551.
(25) Wang, Y. Y.; Fan, D. D.; Liu, J. T.; Chang, Y. P. Clay-mineral compositions of sediments in the Gaoping River-Sea system: Implications for weathering, sedimentary routing and carbon cycling. *Chem. Geol.* **2016**, *447*, 11−26.
(26) Huang, J.; Jiao, W. J.; Liu, J. X.; Wan, S. M.; Xiong, Z. F.; Zhang, J.; Yang, Z.; Li, A.; Li, T. Sediment distribution and dispersal in the southern South China Sea: Evidence from clay minerals and magnetic properties. *Mar. Geol.* **2021**, *439*, 106560.
(27) Cordova-Kreylos, A. L.; Scow, K. M. Effects of ciprofloxacin on salt marsh sediment microbial communities. *ISME J.* **2007**, *1*, 585−595.
(28) Maged, A. L.; Iqbal, J. R.; Kharbish, S. R.; Ismael, I. S.; Bhatnagar, A. M. Tuning tetracycline removal from aqueous solution onto activated 2:1 layered clay mineral: Characterization, sorption and mechanistic studies. *J. Hazard. Mater.* **2020**, *384*, 121320.
(29) Wu, H. H.; Xie, H. R.; He, G. P.; Guan, Y. F.; Zhang, Y. L. Effects of the pH and anions on the adsorption of tetracycline on iron-montmorillonite. *Appl. Clay Sci.* **2016**, *119*, 161−169.
(30) Hacıosmanoğlu, G. G.; Mejias, C.; Martin, J.; Santos, J. L.; Aparicio, I.; Alonso, E. Antibiotic adsorption by natural and modified clay minerals as designer adsorbents for wastewater treatment: A comprehensive review. *J. Environ. Manage.* **2022**, *317*, 115397.
(31) Luo, Y.; Xu, L.; Rysz, M.; Wang, Y. Q.; Zhang, H.; Alvarez, P. J. J. Occurrence and Transport of Tetracycline, Sulfonamide, Quinolone, and Macrolide Antibiotics in the Haihe River Basin, China. *Environ. Sci. Technol.* **2011**, *45* (5), 1827−1833.
(32) Liu, N.; Wang, M. X.; Liu, M. M.; Liu, F.; Weng, L.; Koopal, L. K.; Tan, W. f. Sorption of tetracycline on organo-montmorillonites. *J. Hazard. Mater.* **2012**, *225*−*226*, 28−35.
(33) Zhao, Y. P.; Geng, J. J.; Wang, X.; Gu, X. R.; Gao, S. X. Tetracycline adsorption on kaolinite: pH, metal cations and humic acid effects. *Ecotoxicology* **2011**, *20*, 1141−1147.
(34) Zhang, F. F.; Wang, J. N.; Tian, Y. J.; Liu, C. X.; Zhang, S. Q.; Cao, L. C.; Zhou, Y.; Zhang, S. Effective removal of tetracycline antibiotics from water by magnetic functionalized biochar derived from rice waste. *Environ. Pollut.* **2023**, *330*, 121681.

https://doi.org/10.1021/acsomega.3c06478
ACS Omega 2024, 9, 692−699